Conference on Modelling Fluid Flow (CMFF'25)
The 19th International Conference on Fluid Flow Technologies
Budapest, Hungary, August 26-August 29, 2025

Influence Of Cut-Back Leading Edges On Efficiency And Functionality For An Optimized Semi-Open 2-Channel Impeller

David BECK[1], Paul Uwe THAMSEN[2]

[1] Corresponding Author. Chair of Fluid System Dynamics, Institute of Fluid Mechanics and Technical Acoustics, Technische Universität Berlin. Straße des 17. Juni 135, 10623 Berlin, Germany. Tel.: +49 30 314 70941, E-mail: david.beck@tu-berlin.de
[2] Chair of Fluid System Dynamics, Institute of Fluid Mechanics and Technical Acoustics, Technische Universität Berlin. Straße des 17. Juni 135, 10623 Berlin, Germany. E-mail: paul-uwe.thamsen@tu-berlin.de

ABSTRACT

This publication describes the design of a semi-open 2-channel wastewater impeller, that is optimized for its efficiency with the help of response surface optimization. For the optimal design, a prototype is manufactured out of stainless steel that is able to hold different blade leading edge geometries. For the basic modification, the leading edges from the resulting optimal design from the response surface optimization are examined on the test rig with regard to maximum clear water efficiency and functionality. The functionality is tested with the help of two different test procedures: an optical test to investigate the interaction between duster and impeller with the help of a highspeed camera and an endoscope as well as the long-time functional performance test. Different modifications with cut-back leading edges and different hub designs are designed and are also examined in terms of their maximum clear water efficiency and functionality in order to be able to assess the deviation in maximum efficiencies by gaining functionality. The results show that the efficiency-optimized impeller has a high susceptibility to clogging. The modifications of the leading edges show significant improvements on the functionality by slight reduced efficiencies.

Keywords: clogging, functional performance, optical measurements, optimization, test rig, wastewater pump

NOMENCLATURE

D_{LTF}	$[-]$	degree of long-time functional performance
H	$[m]$	head
P	$[kW]$	mechanical power
Q	$[m^3/h]$	flow rate
m_W	$[g]$	mass of duster
n	$[1/min]$	rotational speed
n_q	$[1/min]$	specific speed
u	$[\%]$	position of leading edge
β	$[°]$	blade angle
η	$[-]$	pump efficiency
ϕ	$[°]$	wrap angle

Subscripts and Superscripts

CW	clear water
H	hub
$L25$	low contamination
$L50$	medium contamination
$MOD0$	modification 0
$MOD1$	modification 1
$MOD2$	modification 2
OP	operating point
S	shroud
h	hydraulic
m	mechanic
$0-60$	averaged over 60 minutes
1	position of leading edge
2	position of trailing edge

1. INTRODUCTION

The demands on wastewater pumps are increasing due to the large number of solids in wastewater. Both high energy efficiency and high availability of wastewater pumps are required [1]. The availability of wastewater pumps is particularly challenged by tear-resistant fibrous materials in wastewater, as these are typical for pump failures [2].

In [3] it was already shown that the efficiency of the entire aggregate has no correlation to the susceptibility to clogging. Furthermore, it was shown that neither the impeller type nor the performance class have an influence on the functionality. Moreover, it has already been shown in [4, 5], that geometric modifications of a wastewater impeller can significantly increase the functionality of wastewater pumps. However, in these previous works, the aim was purely to increase functionality without reference to maintaining maximum efficiency. Within the scope of this publication, the functionality is investigated

accordingly, starting from an efficiency-maximized impeller and optimized by geometric steps to improve the clogging behaviour, whereby the focus is on maintaining maximum efficiency.

2. DESIGN OF OPTIMIZED IMPELLER

The impeller for the investigation is designed as a semi-open 2-channel impeller. For this purpose, a basic impeller is designed, which is then optimized by means of response surface optimization (RSO) to obtain a maximum clear water efficiency. For this basic impeller design, the flow rate Q is selected to 400 m^3/h at a head H of 24 m for the design point. With a design speed n of 1487 min^{-1}, the specific speed n_q results in 45.7 min^{-1}.

In order to be able to estimate the attainable target for the efficiency-optimized impeller, the expected maximum efficiency is first considered. Based on [6], a single stage, single-suction volute casing pump achieves a maximum efficiency for a flow rate Q of 360 m^3/h at a specific speed n_q of 45 min^{-1} a clear water efficiency η_{Pump} of approx. 89 %. As this is a wastewater impeller with only two blades, the efficiency factor according to [7] for 2-channel wastewater impellers is used. This factor varies between 0.8 - 0.98. Therefore, the clear water efficiency η_{Pump} results in an expected efficiency range between 71 and 87 %. However, it should be emphasized that this estimate covers both semi-open and closed 2-channel impellers. Since semi-open impellers have lower efficiencies than closed impellers due to the lack of a shroud and the resulting gap between the tips of the impeller blades and housing, efficiencies up to 80 % are assumed on the test rig.

In addition, boundary conditions are defined for the design impeller that remain unchanged during the RSO. The outlet diameter and the outlet width of the impeller are defined and adapted to the existing volute. This volute is used because previous tests have already shown that its design is not susceptible to clogging. The volute casing has a suction side diameter of 200 mm with a discharge side size of 150 mm. In addition, the impeller is required to have three-dimensional blades that can be varied for both the inner and outer streamlines as part of the optimization process. As the bearing housing for the volute casing is already present, the dimensions of the impeller screw are also predetermined. The blade thickness is 10 mm and is also kept constant across all optimization variants. The blade leading edges for the optimization have an elliptical profile in each sample point.

2.1. Impeller Optimization

For the setup of the RSO, the basic impeller is selected. The volute casing used for the simulation is redesigned based on the existing volute casing and contains the same cross-sectional profile.

The simulations of the basic design and the RSO are carried out as stationary simulations using RANS-equations in a coupled solver with the CFX software. The high resolution scheme is used for numerical discretization and turbulence numerics, using second order central differencing. The SST model is used for turbulence modeling in order to achieve good resolution and convergence both in near-wall areas and free streams [8]. The impeller and the volute casing are meshed with unstructured meshes. The blades as well as the hub of the impeller and the volute casing wall are meshed with prism layers. A dimensionsless wall distance between 30 and 50 is used for the impeller and volute casing, whereby logarithmic wall laws are used. The impeller is calculated as a closed impeller, which means that the gap between the tips of the blades and the frontliner used later in the experiment is not calculated. Furthermore, the impeller back shroud cavity is not considered in the simulation as well. In addition, the domain is given an inlet pipe in front of the suction side of the impeller and an extension on the volute casing. Both pipes are treated as frictionless and are unstructured meshes as well. Stationary coupling models between the rotating impeller and the inlet pupe as well as the volute are used in which the flow variables are transferred axially averaged between the domains. For the convergence criterion, the residuals are set to 10^{-5} by using root mean square (RMS).

For the simulation with the basic impeller and the geometrically similar volute casing, a mesh independence analysis is first carried out, which contains a coarse, a medium and a fine mesh for the impeller. The results for the efficiency are shown in Figure 1.

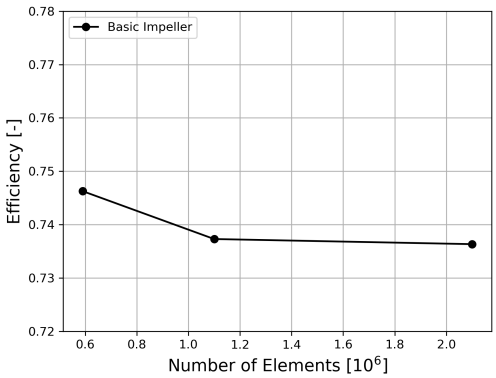

Figure 1. Mesh independence analysis

As can be seen in Figure 1, the deviation between the medium and fine mesh is 0.13 % in efficiency, which is why the medium mesh is used for the RSO. The sample method for the RSO is latin hypercube sampling (LHS). This is due to the fact, that LHS ensures that each parameter is represented in a full manner [9]. For the LHS method, 200 samples are used for the design of experiment (DOE).

A total of ten parameters of the impeller are changed as part of the optimization. Five parameters are selected equally for both the outer (shroud)

and inner (hub) streamline. These include the blade angle of the leading edge β_1 and the blade angle of the trailing edge β_2, the relative starting position of the leading edge u, which influences the diameter of the leading edge accordingly, and, starting from a common baseline, the wrap angle of the leading edge ϕ_1 and the wrap angle of the trailing edge ϕ_2. The parameters vary from the basic design in the direction of both higher and lower values. Figure 2 shows the varied parameters, illustrated using the example of the designed basic impeller for the RSO.

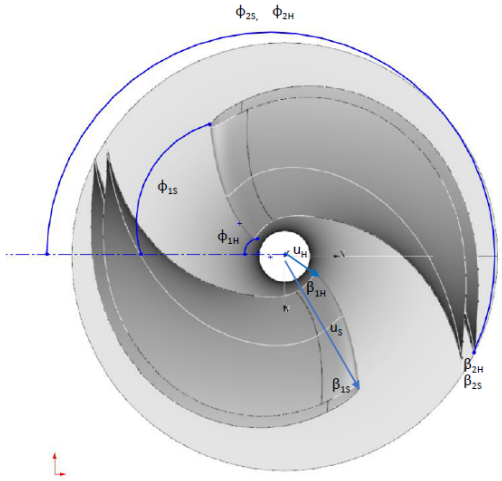

Figure 2. Parameters for DOE

The head H and the efficiency η_{Pump} of the simulated impeller are used as output parameters. The focus here is on maximizing the efficiency, the head plays a subordinate role.

Figure 3 shows the results of the DOE. The sensitivity of the individual varied parameters in relation to the basic impeller with regard to the influence on the efficiency is shown.

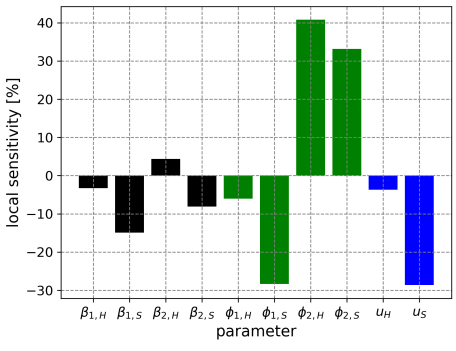

Figure 3. Local sensitivity analsysis for η_{Pump}

Figure 3 shows in particular that increased wrap angles at the outlet ϕ_{2H} and ϕ_{2S} have a significant positive influence on the efficiency of the impeller. In contrast, increased wrap angles at the inlet ϕ_1, especially on the outer streamline ϕ_{1S}, have a negative effect on the efficiency of the basic impeller. The blade angles at the inlet $\beta_{1,H}, \beta_{1,S}$ and outlet $\beta_{2,H}, \beta_{2,S}$ have a subordinate influence. In addition, the position of the leading edge on the outer streamline u_S is decisive for the efficiency of the impeller, while the position of the leading edge on the inner streamline u_H has a minor effect on efficiency. Especially for the outer streamline increased starting positions, which correspond to increased diameters, have a significant reduction in efficiency. This indicates as well, that longer blades, that are starting directly at the suction side of the impeller, are increasing the efficiency for this application.

Based on the individual sample points, it can be seen that particularly high wrap angles lead to high efficiencies. As different blade geometries are to be examined in the further course of the investigations, a target value for a wrap angle at the trailing edge is specified for the optimization in addition to a target value for the maximum efficiency. This wrap angle target value is also selected to be the same for both the inner and outer streamline of the blades, as a two-dimensional trailing edge is desired. The latter is because the use of different blade inlet geometries would otherwise result in unwanted narrow passages between one leading edge and the other blade. The requirements for the optimization are therefore maximizing the efficiency as well as achieving a wrap angle at the trailing edge ϕ_2 of 210° for both streamlines.

For the optimization, the non-dominant sorting genetic alorithm II (NSGA-II) is used as an optimization-algorithm. The selected candidate for optimization meets the boundary conditions of an almost two-dimensional trailing edge with a maximum wrap angle for the end of the blade of approx. 210°. Overall, the impeller has a wrap angle of 189° per blade. In addition, there is a maximum efficiency of 84.2% for the NSGA-II, which results in a simulated efficiency of 83.6% in the geometrically similar volute for the optimization. Due to the range for the estimated efficiency for the semi-open 2-channel impeller, the candidate for the prototype is chosen as the basic modification (MOD 0) for the prototype.

2.2. Prototype Manufacturing

In order to test both the optimized blade geometry and cut-back variants of this blade, a stainless steel prototype is manufactured. This is designed according to the optimized blade contour given by the RSO. In order to be able to test different leading edges in one prototype, the leading edge of the optimized contour for the stainless steel impeller is cut off by 40 % of the outlet diameter and provided with holes on the hub and shroud to which the different leading edges can be screwed as modifications, which are manufactured via 3D-printing. The materials used for the leading edges are polycarbonate (PC) for the optimized blade leading edges (MOD

0) and polylactide (PLA) for the other modifications (MOD 1-2). PC offers increased strength, which is necessary due to the long contour of the optimized blade leading edges, especially regarding the outer streamline. PLA allows fast and cost efficient printing.

To ensure that the impeller has the same gap width of 0.3 mm between the blades and frontliner despite different modifications, an adapter plate is also used, which is screwed onto the back of the stainless steel impeller. This adapter plate holds the shaft-hub connection and represents the same installation situation on the shaft. The frontliner has one groove in all tests, which is used to convey the dusters.

2.3. Impeller Variation

A total of three modifications are used for the impeller in this publication. On the one hand, the blade leading edges resulting from the RSO are used as modification 0 (MOD 0), which form the baseline for the efficiency and functionality measurements. On the other hand, cut-back blade leading edges are implemented, which have the aim of increasing the functionality by slipping off the dusters on the leading edge, while the efficiency is to be maintained. In the first step, the outer streamline of the leading edge is cut-back to 40 % length in relation to the outlet diameter of the impeller, while the inner streamline is unchanged to achieve a resulting curvature between both streamlines. The blade thickness and the elliptical profile remain unchanged. This first modification is continuously described as MOD 1. In addition, starting from MOD 1, the blade leading edges are thickened to 40 mm on the inner streamline in the direction of the impeller screw, which should enable improved slippage. This thickening tapers towards the outer streamline to the thickness of the original blade. In addition, the hub area is reworked to create a plateau between the blades. This plateau is created because previous tests have not only shown severe clogging at the leading edges but also clogging at the screw and hub geometry. This second modification is continuously referred to as MOD 2. Figure 4 shows the individual modifications installed in the stainless steel prototype.

3. TEST SETUP

A clogging test rig at the Chair of Fluid System Dynamics at the Technische Universität Berlin is used for the tests. Three different tests are carried out on this test rig for the various impeller modifications. The first test is a clear water test to record all characteristic values and determine the best efficiency point (BEP). For this purpose, a torque measuring shaft is used on the test rig for the pump in order to record the mechanical power at the pump coupling P_m by measuring the speed with an accuracy of $\pm\,0.05\,\%$ and the torque with an accuracy of $\pm\,0.03\,\%$. Furthermore, a flow meter is used in the pressure pipe of the test rig to measure the flow rate Q with an accuracy of

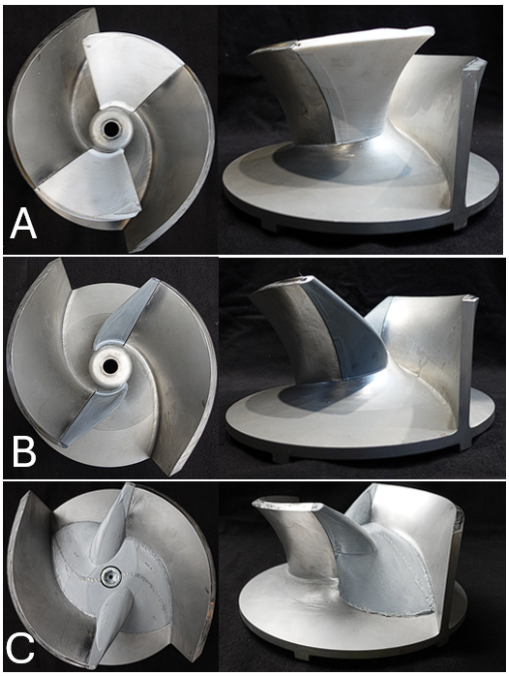

Figure 4. Tested modifications: A) optimized contour MOD 0, B) 40 % cut-back leading edge MOD 1, C) thickened inner streamline MOD 2

$\pm\,0.2\,\%$ and calculate the velocities inside the suction and pressure pipe. A differential pressure sensor with an accuracy of $\pm\,0.5\,\%$ is used to obtain the differential pressure and calculate the head H. With these, the hydraulic power P_h is calculated and the pump efficiency η_{Pump} is calculated with equation 1 [10]:

$$\eta_{Pump} = \frac{P_h}{P_m} \tag{1}$$

The second test is the long-time functional performance test, which is also listed in the DWA-A 120-2 [11] standard. Artificial wastewater is premixed in various contamination classes using tear-resistant dusters. These contamination classes are the low contamination L25, which corresponds to 25 dusters per cubicmeter of water, the medium contamination class L50 with 50 dusters per cubicmeter of water and the high contamination class L100, which represents 100 dusters per cubicmeter of water. Due to the discharge side size of 150 mm for the given volute casing, the tests are carried out with 3 m^3 of water. To carry out the long-time functional performance test, the dry weight of the dusters is determined according to the contamination class. The dusters are inserted into the wastewater tank (WWT). After the dusters have been added, the artificial wastewater is pumped from the WWT back into the WWT for 60 minutes. During the test, the flow rate Q, the head H, the mechanical power P_m and the pump efficiency η_{Pump} are recorded every second. Figure 5 shows the scheme of the long-time functional performance test.

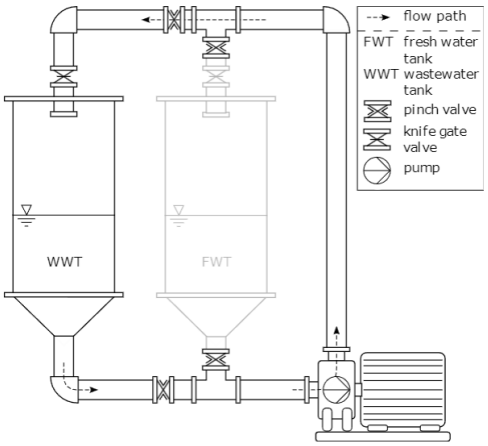

Figure 5. Scheme of the long-time functional performance test [12]

At the end of the 60-minute test period, the pump is switched off, drained and opened. Possible blockages are documented, dried and also weighed. Using the dry weight $m_{W,total}$ added, the weight of the remaining blockages within the pump $m_{W,Pump}$ and the ratio of the average efficiency during the 60-minute test duration $\eta_{test,0-60}$ and the corresponding clear water efficiency at the respective operating point $\eta_{CW,OP}$, the degree of long-time functional performance D_{LTF} is determined according to equation 2.

$$D_{LTF} = \frac{1}{2}\frac{m_{W,total} - m_{W,Pump}}{m_W, total} + \frac{1}{2}\frac{\eta_{test,0-60}}{\eta_{CW,OP}} \qquad (2)$$

A pump is considered to have a low susceptibility to clogging if the D_{LTF} is greater than or equal to 0.7. This value is also the target criterion for the modifications of the prototype impeller in the context of this publication to obtain an impeller with high functionality. The accuracy of the long-time functional performance test is specified according to [13] with an interquartile range of 9 %.

The third test method is an optical measurement, as presented in [14]. For this purpose, a ring made of polymethyl methacylate (PMMA) is connected to the suction side of the pump, which has 8 LED units. Each LED unit has 5595 luminous flux. A polyvinyl chlroide (PVC) ring is also connected in front of the PMMA light ring, which can accommodate a 45° endoscope. In addition, a high-speed camera is connected to the endoscope, which visualizes the interaction between the duster and the impeller at 1000 frames per second. For the tests, 10 dusters per cubic meter of water are used.

These three test procedures are used to evaluate both the efficiency and the functionality of the various modifications.

4. EXAMINATION RESULTS

4.1. Results - Efficiency

Figure 6 shows the results of both the simulated point of the selected optimization candidate with geometrically similar volute and the clear water measurements of MOD 0- MOD 2 on the test rig.

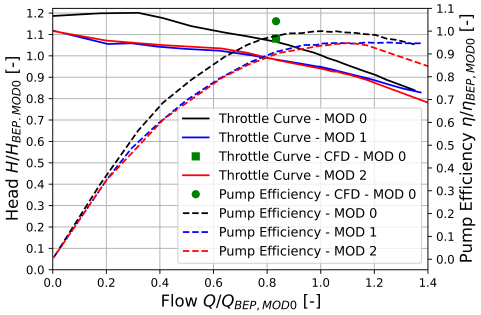

Figure 6. Clear water results for MOD 0-2

When comparing the CFD results for the optimized geometry with a geometrically similar volute to the clear water measurement with the given volute, it is striking that the simulated head of 27.8 m is almost achieved by the clear water measurement for MOD 0. Nevertheless, it can be seen that the simulated efficiency of 83.6 % is not achieved. For the clear water measurement of MOD 0, the BEP has increased in the direction of higher volume flows compared to the design volume flow with a flow rate Q of 480 m^3/h, a head H of 25.7 m and a clear water efficiency of η_{Pump} 80.1 %. Accordingly, the simulated maximum efficiency is relatively 4.4 % above the measured result. This can be related to the assumptions made for the simulation, meaning the use of a stationary simulation without a gap between frontliner and blade tips as well as the lack of the back shroud cavity. In relation to the expected range for maximum efficiency presented in Chapter 2, the results of MOD 0 are within the expected scope.

The clear water results for MOD 1 and MOD 2 each show a reduction in the head H above the flow rate Q due to the shortened blades. In addition, it can be seen that the throttling curves of MOD 1 and MOD 2 are nearly similiar, meaning that the thickening of the inner streamline of the blades and the covering of the impeller screw have a subordinate influence on the hydraulic performance of the impeller in contrast to the blade length. It is also noticeable that cutting back the blade leading edge shifts the BEP of the individual modifications in the direction of higher flow rates. The maximum efficiencies of MOD 1 and MOD 2 are always below the efficiency of MOD 0 due to the modifications of the blade and result in 94.8 % for MOD 1 and 94.9 % for MOD 2 compared to MOD 0. Due to the shift towards higher volume flows, the heads of the two modifications with a shorter blade leading edge are corres-

pondingly lower in the BEP compared to MOD 0, while the mechanical power is higher. Table 1 shows the values of the BEP in relation to MOD 0.

Table 1. BEP results for MOD 0-2

MOD	0	1	2
η/η_{MOD0}	1.000	0.948	0.949
Q/Q_{MOD0}	1.000	1.083	1.104
H/H_{MOD0}	1.000	0.922	0.911
P/P_{MOD0}	1.000	1.050	1.059

4.2. Results - Functionality

For all modifications, the long-time functional performance tests with low contamination L25 in the BEP and optical examinations in the BEP are carried out and compared.

MOD 0: The long-time functional performance test with low contamination for MOD 0 is aborted after approx. 280 seconds of measurement due to a blade breakage of one of the two PC blades. Despite the very short measuring time, a total of 283 g of 283 g of dusters are collected inside the impeller. This results in a $D_{LTF,L25,MOD0}$ of 0.24 with an average normalized pump efficiency during the test of 47.3 %. Even after the short measurement period, this reduced efficiency results from an increase in mechanical power to 111.8 % compared to their clear water value, while the flow rate drops to 78.9 % and the head to 66.1 % compared to the clear water values. The clogging pattern within the impeller after the test and the findings of the optical tests in particular explain why the hydraulically optimized contour is not suitable for media containing fibers. The individual dusters are layered over the leading edges so that subsequent dusters accumulate on them. The blade leading edge, which does not have a sloping edge between the inner and outer streamline, prevents the dusters from slipping off. Figure 7 A) shows an image from the optical test. It can be seen that both blades are covered by dusters. This blockage grows together over the hub area and covers the impeller screw. Figure 7 B) shows the clogging pattern after the long-time functional performance test has been stopped.

MOD 1: The optical tests with 10 dusters per cubic meter show an improved slipping behaviour of the dusters at the leading edges of the blades, as shown in Figure 8.

Figure 8 A) shows a duster that lies on one of the two leading edges. Due to the cut-back of the outer streamline of the blade and the resulting curvature between the outer and inner streamlines, the duster slides along the blade in the direction of the frontliner. Figure 8 B) shows the same experiment after approx. half a revolution. The applied duster has moved in the direction of the outer streamline and ultimately slips towards the suction side of the blade, which shows an improvement compared to MOD 0. However, the optical examinations also show a clogging-prone scenario of MOD 1. Dusters that hit the center of the impeller and thus directly on the hub and on the inner streamline of the blade are not removed and form the beginning of an accumulation. Further arriving dusters are deposited on this initial blockage and grow together over the blades. This initial blockage is shown in Figure 9, in which dusters are attached over the impeller screw and the inner streamline of the blade leading edge and are not discharged until the end of the optical measurement. The low blade thickness on the inner streamline in particular means that there is no slipping behaviour in the optical tests, if the dusters already cover the screw.

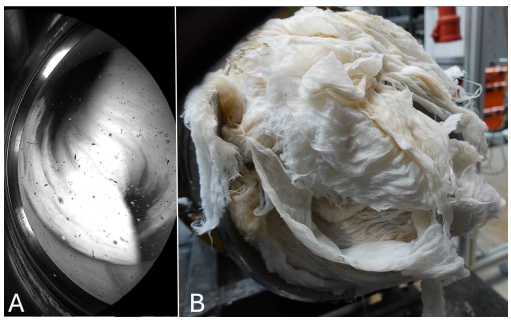

Figure 7. Results for MOD 0. A) accumulation on hub and leading edge during optical investigation, B) blockage inside impeller for L25

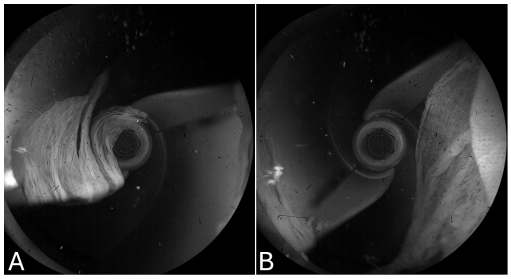

Figure 8. Optical results for MOD 1. A) duster attached on leading edge, B) slipping off duster into channel after half a revolution

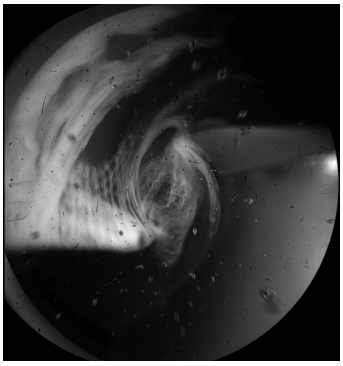

Figure 9. Optical results for MOD 1: clogging on hub, leading edge and impeller screw

This behaviour is also reflected in the long-time functional performance test with low contamination class at BEP. In this test, a total of 221 g of 284 g of dusters are absorbed by the impeller, which corresponds to an improvement compared to the clogging behaviour of MOD 0. Over 60 minutes of measurement, MOD 1 achieves a relative average pump efficiency of 78.9 % compared to clear water operation, which is mainly due to increased mechanical power. This amounts to 115.0 % compared to clear water value, while the volume flow of 97.0 % and the head of 93.5 % are close to the clear water operation. Overall, the $D_{LTF,L25,MOD1}$ is 0.50, which is due to the improved hydraulic performance and the lower absorbed weight during the test. Figure 10 shows the clogged impeller after the end of the long-time functional performance test.

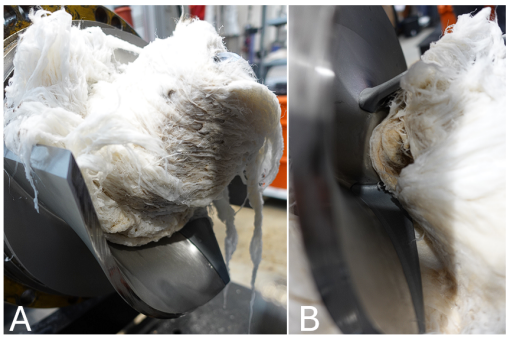

Figure 10. Results for MOD 1: B) accumulation of dusters after completion of test L25, B) accumulation attached to impeller screw

In Figure 10 A) the blockage of 221 g can be seen. Part B) of the figure shows that after lifting the accumulation of dusters, the blockage has grown together over the impeller screw, as could already be observed in the optical examination.

Overall, this results in a gain in functionality of 0.26 for MOD 1, even if this is accompanied by a relative drop in clear water efficiency of 5.2 %, compared to MOD 0.

MOD 2: The optical investigations for MOD 2 show improved slipping behaviour compared to the previous modifications. Figure 11 A) shows two dusters hitting the hub directly. In B), each of these dusters slips into a blade channel after one revolution. The thickened inner streamline of the leading edge helps the dusters to slide either into the blade channel or in the direction of the outer streamline of the leading edge. The plateau, which covers the impeller screw prevents the dusters from sticking on the hub, eventhough a relatively long dwell time of the dusters can be seen during the optical examinations. Due to the flat contour of the plateau, some dusters need several revolutions to be conveyed from the hub towards the channel.

The long-time functional performance test with low contamination L25 in BEP shows a significantly better result compared to the previous modifications. After 60 minutes of measurement, no dusters have accumulated inside the pump. With an average relative efficiency of 95.5 %, this results in a $D_{LTF,L25,MOD2}$ of 0.98 and is therefore above the required 0.7. The mechanical power is unchanged during the test compared to the clear water value, the hydraulic data shows a minimal decrease due to the pumping of the textiles. This results in an average flow rate of 98.6 % and a head of 96.8 % compared to the clear water values.

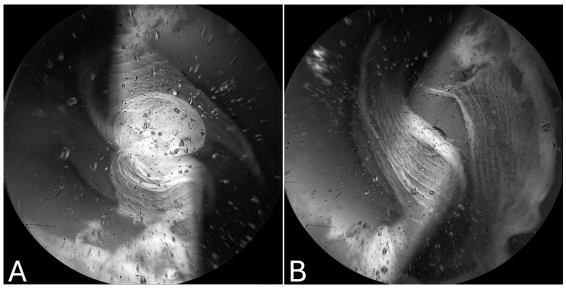

Figure 11. Optical results for MOD 2. A) two incoming dusters on the plateau, B) dusters slipping off into blade channels after one revolution

In addition, due to a result for the $D_{LTF,L25,MOD2}$ greater than 0.7, the long-time functional performance test for MOD 2 is also carried out with medium contamination. In this case, a blockage of 395 g of a total of 572 g of added mass builds up. With an average efficiency over the test duration of 60.7 %, this results in a $D_{LTF,L50,MOD2}$ of 0.46. The flow rate drops to 85.5 % and the head to 75.9 % of the clear water value, while the mechanical performance increases to 107.0 %. Images of the blockages after the end of the test for medium contamination can be seen in Figure 12.

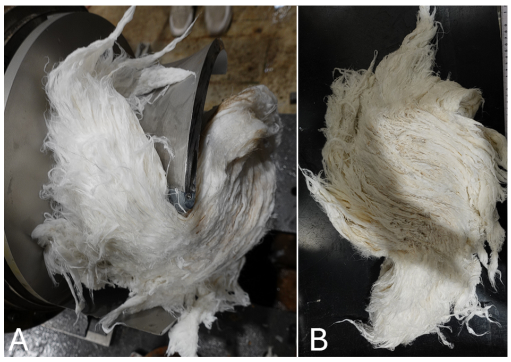

Figure 12. Results for MOD 2: A) clogging inside impeller after completion of test L50, B) removed blockage L50

This behaviour can also be found in the optical tests. Individually arriving dusters slide to the outer streamline, where they are removed by the groove in the frontliner. Due to the fact that only one groove

is used, the dwell time of the dusters on the blades is also too long here. If many dusters hit a blade, an accumulation builds up on the entire leading edge, as can be seen on one blade in the left side of Figure 13. Sliding is no longer possible with this accumulation, so the blockage grows together in the direction of the hub.

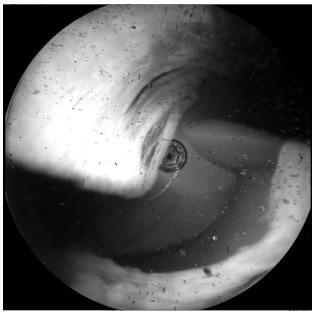

Figure 13. Optical results for MOD 2: clogging scenario on one leading edge

Overall, MOD 2 shows a greatly improved clogging behaviour compared to the previous modifications with a result above the required 0.7 for low contamination while achieving a similiar clear water efficiency compared to MOD 1. In order to further improve the clogging behaviour especially for higher contamination classes, the hub geometry should be further revised to minimize the dwell time of the dusters. In addition, a frontliner with a higher number of grooves should be tested.

5. CONCLUSION

The results of the simulation have shown that the RSO can achieve high efficiencies for wastewater impellers, which are well within the expected efficiency ranges for the corresponding specific speed. However, this flow-optimized contour is highly susceptible to clogging, particularly due to the thin blade leading edges that are strongly exposed to the flow. By cutting back these leading edges, improvements in functionality can already be achieved, but these are accompanied by a moderate drop in efficiency. The thickening of the already cut-back leading edges shows considerable advantages in the slipping behaviour of the dusters, especially in the optical investigations, which also results in an increase in functionality.

REFERENCES

[1] Surek, D., 2014, *Pumpen für Abwasser- und Kläranlagen. Auslegung und Praxisbeispiele*, Springer Vieweg.

[2] Höchel, K., Thamsen, P. U., and Rauwald, H., 2012, "Problem Analysis of sewage pumping stations", *Proceedings of the International Rotationg Equipment Conference*, Düsseldorf, Germany.

[3] Beck, D., Steffen, M., and Thamsen, P. U., 2023, "How to measure the functionality of sewage pumps", *Proceedings of 15th Eurpean Conference on Turbomachinery Fluid dynamics & Thermodynamics*, Budapest, Hungary, Vol. ETC15.

[4] Beck, D., and Thamsen, P. U., 2023, "Development of Sewage Pumps with Numerical and Experimental Support", *International Journal of Turbomachinery Propulsion and Power*, Vol. 8(2).

[5] Beck, D., and Thamsen, P. U., 2024, "Optimization of a Closed 2-Channel Impeller with Experimental and Optical Support", *Proceedings of the ASME 2024 Fluids Engineering Division Summer Meeting*, Anaheim, California, USA, Vol. FEDSM2024.

[6] European Association of Pump Manufacturers, E., 1999, *Attainable efficiencies of volute casing pumps*, Elsevier Science Ltd.

[7] Gülich, J., 2008, *Centrifugal Pumps*, Springer.

[8] Versteeg, H. K., and Malalasekera, W., 2007, *An Introduction to Computational Fluid Dynamics*, Pearson Education Limited.

[9] Mckay, M., Beckman, R., and Conover, W., 2000, "A Comparison of Three Methods for Selecting Values of Input Variables in the Analysis of Output from a Computer Code", *Technometrics*, Vol. 42, No. 1, pp. 55–61.

[10] DIN, 2012, "DIN EN ISO 9906: Kreiselpumpen - Hydraulische Abnahmeprüfungen - Klassen 1,2 und 3", *Tech. rep.*, Deutsches Institut für Normung e.V.

[11] DWA, 2022, "Pumpsysteme außerhalb von Gebäuden - Teil 2: Pumpstationen und Drucksysteme", *Tech. rep.*, Deutsche Vereinigung für Wasserwirtschaft, Abwasser und Abfall e.V.

[12] Brokhausen, F., Herfurth, E., Beck, D., and Thamsen, P. U., 2023, "Exploring characteristics of time-resolved signals in the operation of wastewater pumps", *Proceedings of 15th Eurpean Conference on Turbomachinery Fluid dynamics & Thermodynamics*, Budapest, Hungary, Vol. ETC15.

[13] Pöhler, M., 2020, "Experimentelle Entwicklung eines standardisierten Abnahmeverfahrens für Abwasserpumpen", Ph.D. thesis, Technische Universität Berlin.

[14] Steffen, M., 2023, "Experimentelle Untersuchung der Verstopfungsmechanismen eines Abwasserlaufrades durch Visualisierung der Textil-Laufrad-Interaktion", Ph.D. thesis, Technische Universität Berlin.